Miscible Blends and Block Copolymers. Crystallization, Melting, and Interaction

T. S. Chow

Xerox Webster Research Center, 800 Phillips Road, 0114-39D, Webster, New York 14580.
Received March 30, 1989; Revised Manuscript Received June 12, 1989

ABSTRACT: The effects of crystalline morphology and its kinetics on the melting point depression and thermodynamic interactions in miscible blends are theoretically analyzed and experimentally compared. Two compatible blends are studied: PEO/PMMA and PVF_2/PMMA. As the concentration of amorphous PMMA increases, the thickness of folded-chain lamellae becomes thinner and the rate of crystallization slows down by orders of magnitude. These result in an increase in the concentration-dependent interaction parameter at their melting temperatures. From the morphological and thermal studies of PEO/PS block copolymers, we also find a great deal of similarities in the crystallization, melting, and interaction phenomena between this system and the miscible PEO/PMMA blends.

Introduction

Miscible blends, in which one of their components is crystallizable and the other is amorphous, have been extensively investigated in recent years.[1-14] It was found that the equilibrium melting temperature and crystal growth rate of a semicrystalline blend are depressed as the concentration of amorphous polymer increases. Nishi and Wang (NW)[1] provided an interesting analysis which relates the melting point depression to the polymer–polymer interaction parameter (χ_{12}). Good agreement of the negative χ_{12} values obtained from different experimental techniques was reported.[12-15] However, there are indications that the interaction parameter is not a constant but depends on concentration.[12-17]

It is the purpose of this paper to analyze the effects of crystalline morphology and its kinetics on the melting point depression and thermodynamic interaction in miscible polymer blends by extending the NW equation. Two compatible blends are studied: PEO/PMMA and PVF_2/PMMA, where PEO = poly(ethylene oxide), PMMA = poly(methyl methacrylate), and PVF_2 = poly(vinylidene fluoride). In the study of PEO/PS block copolymers, where PS = polystyrene, it has been observed[18,19] that PS molecules are incorporated in the interlamellar regions of PEO spherulites as depicted in Figure 1. Such morphology is similar to that which was observed in the miscible PEO/PMMA blends.[9,14] Other similarities between the two systems will also be discussed.

Thermodynamic Consideration

According to Flory's theory of melting point depression,[20] the equilibrium melting temperature of a miscible polymer blend is determined by the condition that the chemical potentials of crystalline component in the crystalline and liquid phases must be equal, i.e.

$$\mu_2 - \mu_2^\circ = \mu_2^c - \mu_2^\circ \tag{1}$$

The chemical potential μ_2 per mole of crystallizable units in the blend relative to its chemical potential μ_2° in the pure liquid state is[1,20,21]

$$\mu_2 - \mu_2^\circ = \frac{RTV_2}{V_1}\left[\frac{\ln \phi_2}{N_2} + \left(\frac{1}{N_2} - \frac{1}{N_1}\right)\phi_1 + \chi_{12}\phi_1^2\right] \tag{2}$$

where V is the molar volume of repeating polymer unit, N is the degree of polymerization, ϕ is the volume fraction, R is the gas constant, T is the absolute temperature, the subscript 1 refers to the amorphous polymer and 2 to the crystalline polymer.

In general, the free energy of crystallization from the melt can be written as[22,23]

$$\Delta G = G_{cryst} - G_{melt} \tag{3}$$

The free enthalpy of a crystal consists of bulk and surface contributions

$$G_{cryst} = G_{bulk} + \sum_i \gamma_i A_i \tag{4}$$

where γ_i represents the surface free energy per unit area and A_i is the corresponding surface area. The surface area energies are always positive and $G_{melt} - G_{bulk}$ is greater than zero for temperature below the melting point. Thus, the difference in the chemical potential between a crystalline polymer repeating unit μ_2^c and the same unit in the liquid state becomes

$$\mu_2^c - \mu_2^\circ = V_2\Delta G/V_c = V_2(\Delta g_2 + 2\gamma_e/l) \tag{5}$$

where V_c is the crystal volume. The bulk related free enthalpy per unit volume is given by the familiar expression

$$\Delta g_2 = -\Delta h_2(1 - T/T_m^\circ) \tag{6}$$

where Δh_2 is the heat of fusion per unit volume of a crystal and T_m° is the melting point of a pure polymer. Considering a two-dimensional nucleation consistent with the morphological picture depicted in Figure 1, we have

$$2\gamma_e/l \simeq \sum_i \gamma_i A_i/V_c \tag{7}$$

where γ_e is the interfacial energy per unit area for the fold surface shown in Figure 2, l is the lamellar thickness, and $V = abl$ with a fixed monomolecular layer b.

By substituting eq 2 and 5–7 into eq 1 and by replacing T by T_m, the equilibrium melting temperature for the blend, one obtains

$$\frac{T_m}{T_m^\circ} = \frac{1 - 2\gamma_e/l\Delta h_2}{1 - \dfrac{RT_m^\circ}{V_1\Delta h_2}\left[\dfrac{\ln \phi_2}{N_2} + \left(\dfrac{1}{N_2} - \dfrac{1}{N_1}\right)\phi_1 + \chi_{12}\phi_1^2\right]} \tag{8}$$

To an approximation sufficiently accurate for N_1 and N_2 much larger than 1 and at low to moderate $T_m^\circ - T_m$, eq 8 reduces to

$$\frac{T_m}{T_m^\circ} \simeq 1 - \frac{2\gamma_e}{l\Delta h_2} + \frac{RT_m^\circ}{V_1\Delta h_2}\chi_{12}\phi_1^2 \tag{9}$$

0024-9297/90/2223-0333$02.50/0

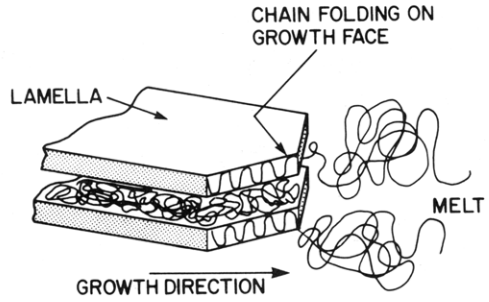

Figure 1. Schematic representation of chain-folding crystallization in a polymer mixture.[19]

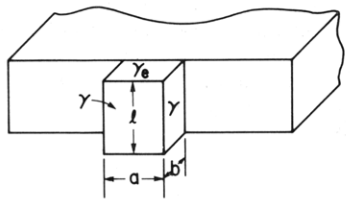

Figure 2. Model for surface nucleation and crystallization.

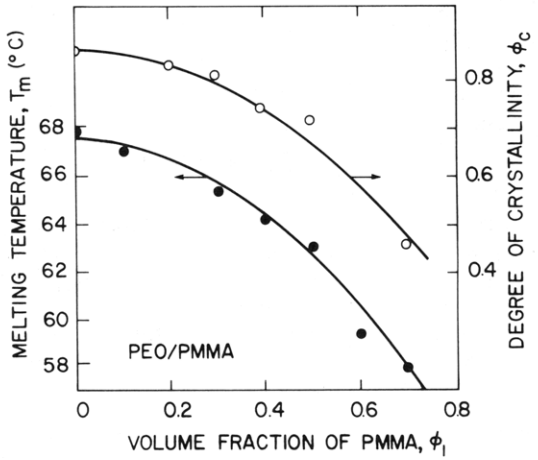

Figure 3. Dependence of melting temperature and degree of crystallinity of PEO/PMMA on the volume fraction of PMMA. Circles are experimental;[9] curves are fitted to eq 13 and 14.

The main difference between the above equation and the NW equation is that the second term on the right, eq 9, relates the melting point not only to the interaction parameter but also to crystal thickness or perfection.

The free energy for crystallization per unit volume may also be approximated as follows[4,24]

$$\Delta g = \Delta G/V_c = -\Delta h_2(1 - T/T_m^\circ)\phi_c \qquad (10)$$

where ϕ_c is the degree of crystallization. From eq 5–10, we obtain

$$1/l = a\Delta h_2(1 - \phi_c)\phi_1^2/2\gamma_e \qquad (11)$$

and

$$\chi_{12} = -aV_1\Delta h_2\phi_c/RT_m^\circ \qquad (12)$$

where

$$a = (T_m^\circ - T_m)/T_m^\circ\phi_1^2 \qquad (13)$$

The above equations are the functional relationships between the melting point depression, lamellar thickness, and polymer–polymer interaction parameter.

Miscible Blends

The crystallization and melting behavior of solution-cast films of PEO/PMMA blends were measured as a function of composition.[9] Using the reported data and eq 13, we find that a is a composition-independent constant. The measured degree of crystallinity can be expressed in the form

$$\phi_c = \phi_c^\circ - \beta\phi_1^2 \qquad (14)$$

with the constants ϕ_c° and β determined from the data in Figure 3. In addition to T_m°, a, ϕ_c°, and β, other useful properties (V_1, Δh_2, ρ_1, and ρ_2) are listed in Table I. The density ratio (ρ_1/ρ_2) is needed in relating the weight (w_1) to volume fractions, i.e.

$$w_1 = (\rho_1/\rho_2)\phi_1/[1 + (\rho_1/\rho_2)\phi_1] \qquad (15)$$

Table I
Parameters for Thermal Analysis

	PEO/PMMA	PVF_2/PMMA	PEO/PS solvent	PEO/PS melt
V_1, cm^3/mol	83.4	84.9	101.0	
Δh_2, cal/cm^3	57.3[a]	44.0	52.7[b]	
T_m°, °C	67.5[a]	170.6	59.3[b]	
a	0.057	0.068	0.038	
ϕ_c°	0.86	0.96	0.95	0.86
β	0.79	0.52	0.59	0.63

[a] From ref 9 and 18. [b] From ref 19 and 24.

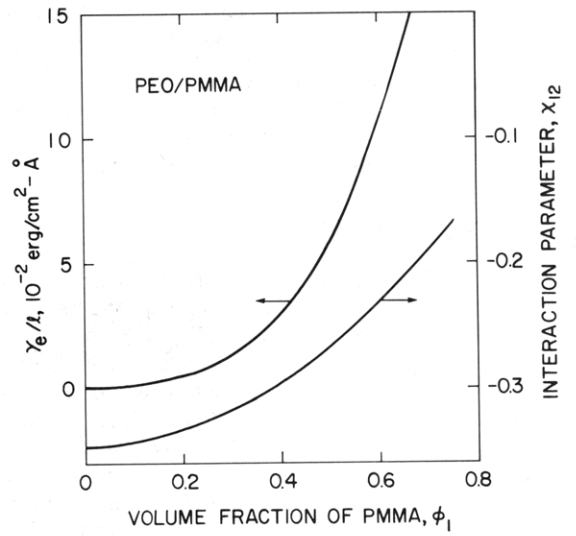

Figure 4. Concentration-dependent lamellar thickness and interaction parameter in PEO/PMMA.

In Figure 4, the changes of lamellar thickness and interaction parameter in PEO/PMMA blends are calculated from eq 11 and 12. As the volume fraction of the crystallizable PEO decreases from 100% to 30%, we find that the lamellar thickness becomes thinner and less perfect, which is in agreement with what had been seen under electron microscope.[9] At the same time, the polymer mixture becomes less compatible, which is also consistent with the reported observation.[8,14]

The thermal and crystallization behavior of PVF_2/PMMA can also be described by eq 13 and 14 with the parameter T_m°, a, ϕ_c°, and β determined from the experimental data[1] and shown in Table I. The dependence of PVF_2 crystal thickness l and interaction parameter χ_{12} on the volume fraction of PMMA is calculated in Figure 5. The composition-dependent χ_{12} parameter for this system was mentioned by other authors.[12-17] The present analysis supports this notion as a general phenomenon for crystallizable miscible blends and quantifies the contribution from the change in crystalline structure on the composition-dependent χ_{12} parameter.

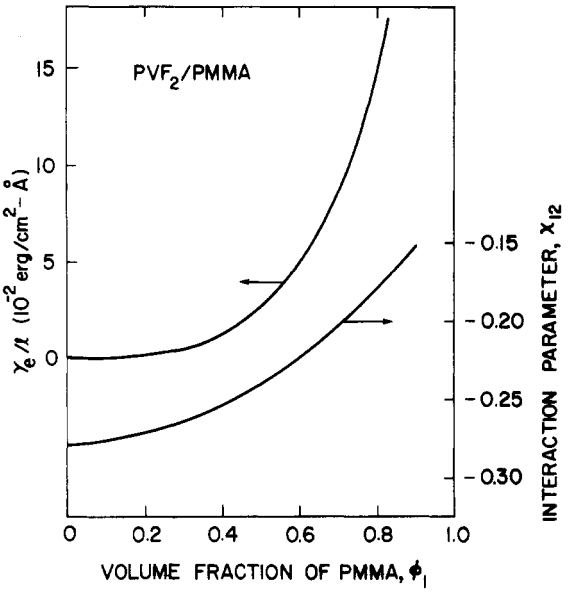

Figure 5. Concentration-dependent lamellar thickness and interaction parameter in PVF_2/PMMA.

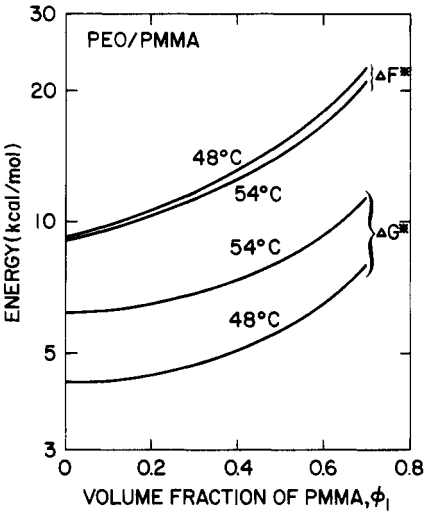

Figure 6. Effects of composition and temperature on the critical free energy of crystallization (ΔG^*) and activation energy for molecular transport (ΔF^*) in PEO/PMMA.

Crystallization Kinetics

In addition to the above-mentioned thermodynamic properties, the presence of an amorphous polymer should have a strong effect on the spherulitic crystallization in compatible blends.[3] The steady-state growth rate, $\dot{r} = dr/dt$ with r = the radius of spherulite, is governed by a modified Turnbull–Fisher equation in the form[22,25,26]

$$\dot{r} = \dot{r}_0 \exp[-(\Delta G^* + \Delta F^*)/RT] \tag{16}$$

where ΔG^* is the free energy of crystallization of a nucleus of critical size, ΔF^* is the activation energy controlling the short-distance diffusion of crystallizing element across the phase boundary, and $\dot{r}_0$ is a constant. Following the physical picture depicted in Figures 1 and 2 and eq 3 and 4, the critical value of ΔG is

$$\Delta G^* = \frac{4b\gamma\gamma_e}{\Delta g_2} = \frac{4b\gamma\gamma_e T_m^\circ}{T(T_m^\circ - T)\phi_c} \tag{17}$$

The mobility of chain segments is inversely proportional to the local relaxation time, λ, which is related to the free-volume fraction, f, by Doolittle's equation[27,28] as

$$\lambda \sim \exp(1/f) \tag{18}$$

At temperatures above the glass transition temperature (T_g), the free-volume fraction can be approximated by the "universal" relation

$$f = a_f(T - T_0) \tag{19}$$

where the thermal coefficient of expansion of free volume $a_f = 4.8 \times 10^{-4}$/°C and $T_0 = T_g - 51.6$ °C. Comparing eq 16 and 19, we have

$$\Delta F^* = 2080RT/(T - T_g + 51.6) \tag{20}$$

From the T_g data of PEO/PMMA blends,[8] the glass transition temperature for this system can be adequately described by[29]

$$1/T_g = w_1/T_{g1} + (1 - w_1)/T_{g2} \tag{21}$$

The critical free energy of crystallization and the activation energy for molecular transport in PEO/PMMA blend are plotted in Figure 6 as a function of the volume fraction of PMMA and crystallization temperature. In addition to those given in Table I, parameters listed in Table II are used in the calculation. When the concentration of PMMA increases, Figure 6 reveals that the PEO crystal becomes more difficult to form and, at the same time, the energy barrier for a molecule to diffuse across the liquid–crystal interface gets higher. Therefore, the growth rate of spherulites in the PEO/PMMA blends slows down as the volume fraction of PMMA goes up in Figure 7.

A clear physical picture emerges from the thermodynamic and kinetic analyses. When the volume fraction of PEO decreases from 100% to 30%, the basic interlamellar structure depicted in Figure 1 is not altered,[9] but the local population and motion for the crystalliz-

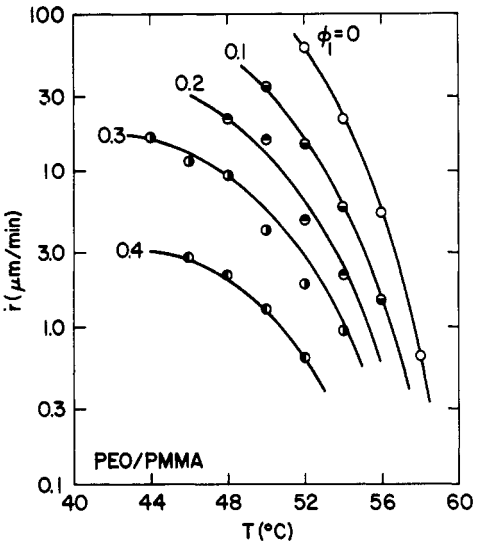

Figure 7. Comparison of calculated (—) and measured[11] (circles) radial growth rate of spherulites in PEO/PMMA as a function of composition and crystallization temperature.

Table II
Additional Parameters for Crystallization Kinetics

	PEO/PMMA	PVF_2/PMMA
b, Å	4.65	4.45
$\gamma\gamma_e$, erg^2/cm^4	190	220
ρ_1, g/cm^3	1.20	1.20
ρ_2, g/cm^3	1.17	1.80
T_{g1}, °C	100	100
T_{g2}, °C	−45	−47

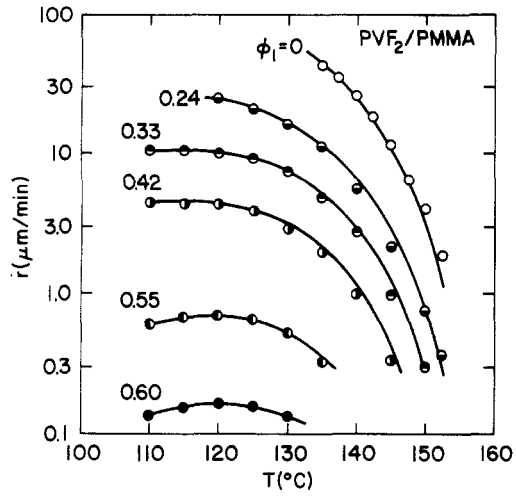

Figure 8. Comparison of calculated (—) and measured[3] (circles) radial growth rate of spherulites in PVF_2/PMMA as a function of composition and crystallization temperature.

Table III
Composition Dependent Constant $\dot{r}_o$

	PEO/PMMA					
ϕ_1	0.0	0.1	0.2	0.3	0.4	
log $\dot{r}_o$ ($\dot{r}_o$, μm/min)	11.50	11.38	11.60	12.10	12.60	
	PVF_2/PMMA					
ϕ_1	0.0	0.24	0.33	0.42	0.55	0.60
log $\dot{r}_o$ ($\dot{r}_o$, μm/min)	7.65	7.43	7.30	7.20	7.00	6.65

able PEO and amorphous PMMA to interact are significantly reduced. These result in orders of magnitude drop in the rate of crystallization, in thinning the thickness of lamellae, and in smaller negative values of the polymer–polymer interaction parameter. The blends become less compatible.

Equations 16–21 should apply equally well to other miscible blends. Consider the PVF_2/PMMA blends. When the experimental spherulitic growth rate versus crystallization temperature data for a given volume fraction of PMMA are used, the values for b and $\gamma\gamma_e$ are determined as shown in Table II. The other required input data are given in Table I. A comparison between the calculated and measured[3] radial growth rate of spherulites in PVF_2 and its blends with PMMA at various compositions and temperatures is carried out in Figure 8. Our analysis reveals that all the physical properties and parameters listed in Tables I and II are independent of temperature and composition. In order to achieve the quantitative comparisons shown in Figures 7 and 8, Table III suggests that the constant $\dot{r}_o$ is independent of temperature but is a function of composition.

Block Copolymers

The melting point depression has not been considered in previous theories on the block copolymers with crystallizable block.[30,31] The theory proposed in this paper will be used to describe the phenomenon. From the morphological and thermal studies of PEO/PS block copolymers,[18,19] the results indicated: (1) the PEO folded-chain lamellae are sandwiched between the amorphous PS layers depicted in Figure 1 and (2) the size and perfection of the lamellae appear to depend on copolymer composition. The lamellae thickness becomes thinner, and the lamellae becomes progressively more distorted, as the volume fraction of PS increased from 0 to 70%.

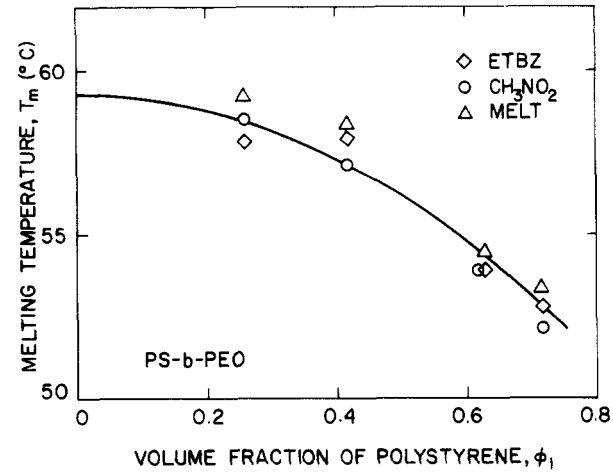

Figure 9. Melting point depression in PEO/PS block copolymer films cast from solvents and melt. Symbols are experimental;[19] curve is fitted to eq 13.

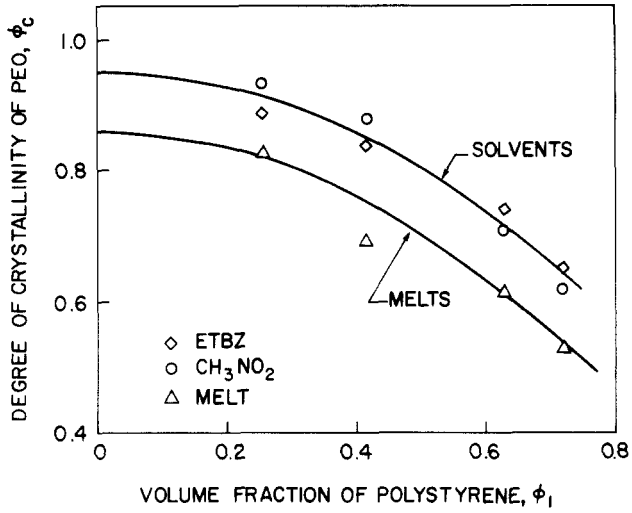

Figure 10. Degree of crystallinity of PEO versus volume fraction of PS. Symbols are experimental;[19] curves are fitted to eq 14.

These are the same conclusions reached for the miscible PEO/PMMA blends mentioned earlier. However, a block copolymer, in which the incompatible components are linked through covalent bonds, differs from a mixture of compatible homopolymers. Covalent bonding can significantly improve the miscibility of polymer components in block copolymers which could be characterized by the χ_{12} parameter.

Figure 9 shows that the melting point depression data for PEO/PS copolymer films casted from preferential solvents and the melt[19] can indeed be described by eq 9 or 13 plotted as the solid curve, from which T_m^o and a are determined. A comparison of eq 14 with the measured degree of crystallinity as a function of the volume fraction of PS is shown in Figure 10. The method of sample preparation seems to have an effect on the values of ϕ_c but has no influence on the functional relationship between ϕ_c and ϕ_1. When the parameters listed in Table I for PEO/PS block copolymers are used, the changes in the thickness of lamellae and interaction parameters are illustrated in Figures 11 and 12, respectively, as a function of PS concentration. The theoretical predictions are consistent with the experimental observations[19] mentioned earlier. While an increase in the volume fraction of the amorphous component affects the melting behavior and the crystal thickness in a similar way in both copolymer

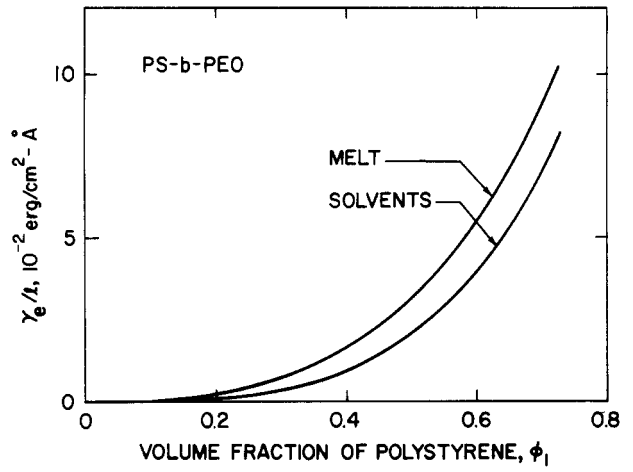

Figure 11. Composition-dependent lamellar thickness in PEO/PS.

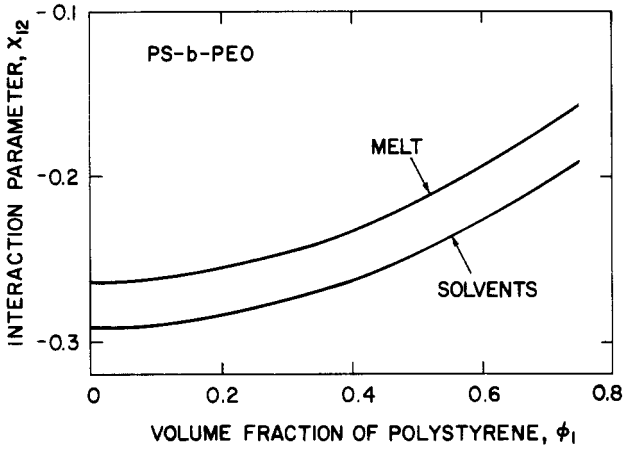

Figure 12. Composition-dependent interaction parameter in PEO/PS.

and blend systems, we should also mention that kinetics (such as thermal annealing) plays a much more important role in crystallizable homopolymers[23] than in crystallizable block copolymers.[31]

Conclusions

The well-known Nishi–Wang equation for the melting point depression of miscible polymer blends has been extended to include the effect of crystalline morphology. When the basic structure of folded-chain lamellae sandwiched between amorphous polymer layers remains unaltered, the melting point depression arises, not only from the polymer–polymer interaction but also from the change in crystal thickness or perfection. We find that the thickness of lamellae becomes thinner and the negative value of the χ_{12} parameter smaller at low concentrations of the crystallizable component in miscible blends.

Without changing the input parameters, the composition and temperature dependences of spherulitic growth rates of the PEO/PMMA and PVF_2/PMMA blends are theoretically calculated and experimentally compared. As the volume fraction of PMMA increases, the local population and motion for the crystallizable and amorphous components to interact are significantly reduced. These results in orders of magnitude drop in the rate of crystallization. The polymer mixtures become less compatible, which is consistent with the reported observations.

By comparing the morphological and thermal behavior of the PEO/PS block copolymers with those of the PEO/PMMA miscible blends as a function of composition, we find a great deal of similarities in the crystallization, melting, and interaction phenomena between these two systems. The basic PEO lamellar structure in PEO/PS copolymers is preserved, but the thickness or perfection of lamellae decreases, as the volume fraction of PEO decreases from 0 to 70%. Therefore, an increase in the concentration-dependent interaction parameter at the melting temperatures results.

Registry No. PEO, 25322-68-3; PMMA, 9011-14-7; PVF_2, 24937-79-9; (PEO)(PS) (block copolymer), 107311-90-0.

References and Notes

(1) Nishi, T.; Wang, T. T. *Macromolecules* **1975**, *8*, 909.
(2) Kwei, T. K.; Patterson, G. D.; Wang, T. T. *Macromolecules* **1976**, *9*, 780.
(3) Wang, T. T.; Nishi, T. *Macromolecules* **1977**, *10*, 421.
(4) Paul, D. R.; Barlow, J. W. In *Polymer Alloys II*; Klempner, D., Frisch, K. C., Eds.; Plenum Press: New York, 1980; p 239.
(5) Imken, R. L.; Paul, D. R.; Barlow, J. W. *Polym. Eng. Sci.* **1976**, *16*, 593.
(6) Morra, B. S.; Stein, R. S. *J. Polym. Sci., Polym. Phys. Ed.* **1982**, *20*, 2243.
(7) Aubin, M.; Prud'homme, R. E. *Macromolecules* **1980**, *13*, 365.
(8) Li, X.; Hsu, S. L. *J. Polym. Sci., Polym. Phys. Ed.* **1984**, *22*, 1331.
(9) Martuscelli, E.; Silvestre, C.; Addonizio, M. L.; Amelino, L. *Makromol. Chem.* **1986**, *187*, 1557.
(10) Rim, P. B.; Runt, J. P. *Macromolecules* **1984**, *17*, 1520.
(11) Calahorra, E.; Cortazar, M.; Guzman, G. M. *Polymer* **1982**, *23*, 1322.
(12) Hadziioannou, G.; Stein, R. S. *Macromolecules* **1984**, *17*, 567.
(13) Alfonso, G. C.; Russell, T. P. *Macromolecules* **1986**, *19*, 1143.
(14) Ito, H.; Russell, T. P.; Wignall, G. D. *Macromolecules* **1987**, *20*, 2213.
(15) Riedl, B.; Prud'homme, R. E. *Polym. Eng. Sci.* **1984**, *24*, 1291.
(16) Wendorff, J. H. *J. Polym. Sci., Polym. Lett. Ed.* **1980**, *18*, 439.
(17) DiPaola-Baranyi, D.; Fletcher, S. J.; Degré, P. *Macromolecules* **1982**, *15*, 885.
(18) Kovacs, A. J.; Lotz, B. *Kolloid Z. Z. Polym.* **1966**, *209*, 97.
(19) O'Malley, J. J.; Crystal, R. G.; Erhardt, P. F. In *Block Copolymers*; Aggarwal, S., Ed.; Plenum Press: New York, 1970; p 163.
(20) Flory, P. J. *Principles of Polymer Chemistry*; Cornell University Press: Ithaca, NY, 1953; p 568.
(21) Scott, R. L. *J. Chem. Phys.* **1949**, *17*, 279.
(22) Wunderlich, B. *Macromolecular Physics*; Academic Press: New York, 1976; Vol. 2.
(23) Chow, T. S. *Macromolecules* **1981**, *14*, 1386.
(24) Mandelkern, L. *Crystallization of Polymers*; McGraw-Hill: New York, 1964.
(25) Turnbull, D.; Fisher, J. C. *J. Chem. Phys.* **1949**, *17*, 71.
(26) Hoffman, J. D.; Weeks, J. J. *J. Chem. Phys.* **1962**, *37*, 1723.
(27) Chow, T. S. *J. Rheol.* **1986**, *30*, 729.
(28) Doolittle, A. K. *J. Appl. Phys.* **1951**, *22*, 1471.
(29) Fox, T. G.; Loshaek, S. *J. Polym. Sci.* **1955**, *15*, 371.
(30) DiMarzio, E. A.; Guttman, C. M.; Hoffman, J. D. *Macromolecules* **1980**, *13*, 1194.
(31) Whitmore, M. D.; Noolandi, J. *Macromolecules* **1988**, *21*, 1482.